

Harnessing Sustainable Energy: Pico-Hydro Power Generation Using an Undershoot Water Wheel Turbine in Irrigation Canals

Iftitah Imawati✉, Galang Ismu Kurniawan, Muhammad Rifan Ghifari, Muhammad Nauval, Fajar Arisandi, Hendra Setiawan, Husein Mubarak

Electrical Engineering Department of Universitas Islam Indonesia, Jalan Kaliurang Km14, Sleman, 55584, Indonesia

✉Corresponding Author: iftitah.imawati@uii.ac.id | Phone: +62 821-3853-2134

Received: 17 May 2025

Revision: 18 July 2025

Accepted: 28 August 2025

Abstract

With the increasing demand for electricity and environmental concerns related to the use of fossil fuels, the need for renewable energy solutions is becoming increasingly important. The potential of hydropower generation needs to be harnessed for daily electricity needs. The proposed system harnesses the flow of water in irrigation channels, using turbines made of galvanized plates and plastic to generate electricity for small-scale applications such as street lighting. To overcome the challenges of manual monitoring, especially during the rainy season, an IoT-based monitoring tool is included. This tool allows remote tracking of system performance, including generator output, battery voltage, and load current, through an internet-connected smartphone interface, allowing for real-time monitoring. Laboratory and field tests were conducted in Yogyakarta, Indonesia. The system demonstrated the ability to produce stable voltage and power, achieving an efficiency of 11.38%. The system demonstrated a data transmission delay of 5.64 seconds via Blynk, with a recorded power consumption of 2,231 watts. The sensor readings showed high accuracy, with generator voltage accuracy of 99.33% and load current accuracy of 99.26%.

Keywords: Pico-Hydro, Renewable Energy, IoT, Turbine, Irrigation Canals

Introduction

In Indonesia, irrigation canals are extensively distributed across various regions, representing a largely untapped resource for renewable energy generation (Usmani et al., 2021). According to data from the Ministry of Public Works and Public Housing (PUPR), Indonesia boasts over 7.2 million hectares of rice fields serviced by irrigation systems, encompassing thousands of kilometers of primary, secondary, and tertiary canals that transport water from its sources to agricultural lands (de Zoete, 2024). Furthermore, it has been reported that there are approximately 89,000 kilometers of irrigation canals dedicated to watering agricultural fields across the country (Ashour et al., 2023), (W. V. Siregar, Hasibuan, Hidayatullah, et al., 2024). The water discharge rates from these irrigation systems vary significantly depending on location, season, and climatic conditions, typically ranging from 0.3 to 1 liter per second per hectare of rice field. During the rainy season, water flow can increase substantially, whereas it tends to decrease in the dry season (Quang et al., 2024). The Directorate General of Water Resources indicates that the average water discharge through the primary irrigation systems in certain regions of Indonesia is around 10 to 20 cubic meters per second, with larger canals in areas such as Java and Bali often experiencing higher flow rates to meet the greater agricultural water demands (Hadian et al., 2024), (Hasibuan et al., 2023).

The prevailing irrigation methods in Indonesia primarily utilize the potential energy from flowing water (Tirtalistyani et al., 2022). In addition to serving agricultural needs, these canals present an opportunity to integrate mini pico-hydro power generation systems, harnessing the flowing water's energy to produce electricity without disrupting their primary function of irrigation (Abdou & Abdou, 2024). Installing pico-hydro power generation systems in irrigation canals capitalizes on existing infrastructure, resulting in low-cost renewable energy generation with minimal environmental impact (Ma et al., 2025). This system is particularly advantageous for rural areas, providing reliable and sustainable energy access that supports agricultural operations while enhancing energy independence and empowering local communities (Emezirinwune et al., 2024). By leveraging irrigation water flow, pico-hydro optimizes water resource utilization, diminishes reliance on fossil fuels, and contributes to reducing energy poverty in rural regions (Calimpusan et al., 2024).

The undershoot water wheel turbine is selected for this application due to its efficient operation at low water flows and minimal head requirements, making it well-suited for irrigation canal conditions (Teodoro, 2024), (W. V. Siregar, Hasibuan, Daud, et al., 2024). Its simple and durable design facilitates installation and maintenance, especially in remote areas, while being environmentally friendly by maintaining the natural flow of water and aquatic life (Koondhar et al., 2024). To maximize efficiency and reliability, real-time monitoring of system performance, which is highly dependent on flow conditions, turbine placement, and environmental factors, is essential (Firoozi et al., 2024), (Kurniawan et al., 2021). This is where Internet of Things (IoT) technology plays a pivotal role (Rath et al., 2024). IoT enables remote monitoring and management of pico-hydro systems, optimizing energy production, facilitating early problem detection, and ensuring better integration with broader energy networks (Sumarjo et al., 2024), (Hasibuan et al., 2024).

IoT technology allows physical devices or hardware to connect to the internet and communicate with one another, enabling periodic information gathering on key metrics such as voltage, current, and power output from the pico-hydro plant (Y. Siregar et al., 2024). Sensor readings can be processed using Arduino for monitoring purposes. Previous studies have demonstrated effective monitoring systems where data from sensors is sent to applications like Ubidots for real-time information on power generation performance (Balamanikandan et al., 2024). For instance, a project conducted in Nepal successfully implemented a pico-hydro system integrated with IoT technology to enhance monitoring and efficiency in rural electrification (Kandasamy et al., 2025). The system demonstrated a significant increase in energy access for local communities while ensuring sustainable energy production. This project highlights the potential of similar systems in utilizing existing water infrastructure for renewable energy generation (Kurniawan et al., 2022). For instance, remote control of lighting systems can enhance user convenience by eliminating the need for manual switching, as demonstrated in projects utilizing applications like Blynk to manage lighting via smartphones. In the pico-hydro system, a battery stores energy from the generator's conversion, and to easily determine the battery's capacity, voltage and current sensors can be integrated to measure the input and output values. These readings are processed through a microcontroller program, and the results are transmitted to a web monitoring interface to provide insights into battery capacity as voltage levels. The system will consist of two subsystems: the pico-hydro generation system and the IoT monitoring system.

Materials & Methods

1. Integration of Systems

Integration the whole system can be shown in block Figure 1. The power generation power system as there are sensors to measure DC voltage and current from picohydro and battery. After obtaining the values of these two parameters, the power value generated by the PLTPH and the capacity of the PLTPH storage battery can be known. The microcontroller is used to process data taken from the sensor. Through a wireless communication module, the processed data from the microcontroller will be sent to the web server to be displayed and stored in the database. The display of monitoring the performance of picohydro and battery percentage can be accessed via smartphone. Furthermore, the output produced by the voltage and current sensors from each measurement, namely picohydro performance and battery percentage, is displayed in real-time and there is a relay control of the load remotely.

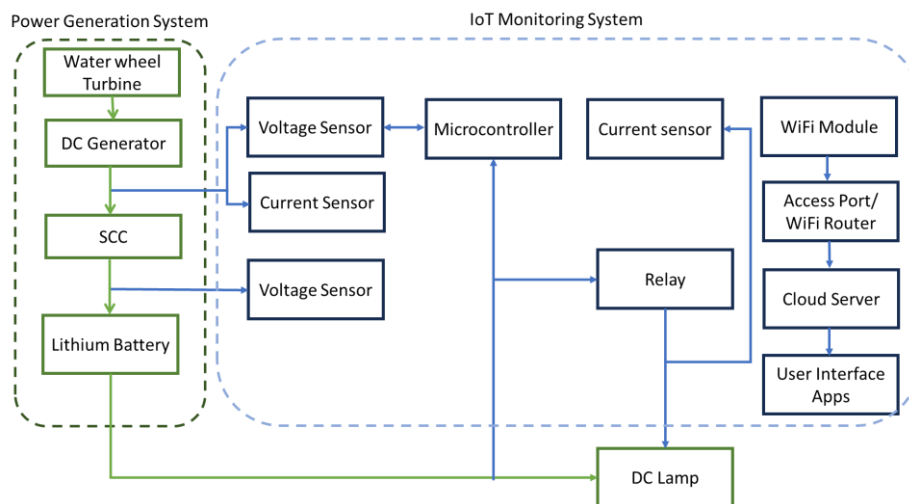


Figure 1. Integration the Whole System

2. Pico-Hydro Power Generation System

The pico hydro power generation sub system have two major components consists of frame and turbine, and the electrical control panel. The overall system design process are based on the calculation. Pico-hydroelectric power plants essentially harness the difference in elevation and the volume of water flow per second from sources such as irrigation, rivers, or waterfalls. This flow of water turns the turbine shaft to generate mechanical energy. This mechanical energy then powers the generator, which produces electricity that is stored in a battery. Water discharge (Q) refers to the flow rate of liquid passing through a given cross-section over time and is determined by the velocity (V) and area (A), typically measured in meter cubic per second, as expressed in Equation (1)

$$Q = V \times A \quad (1)$$

Velocity of water flow and area can be measured with Equation (2) and Equation (3), with distance (d) and time (t) and irrigation width (I) and irrigation depth (D).

$$V = \frac{d}{t} \quad (2)$$

$$A = I \times D \quad (3)$$

Hydroelectric capacity can be calculated with water flow rate. Water flow rate is a key factor to hydroelectric capacity. The parameters are water density ($\rho = 0.998 \text{ g/cm}^3$), gravity. And head [3]. Hydroelectric capacity can be calculated using

the Equation (4).

$$Q = \rho \times g \times Q \times h \tag{4}$$

Turbine rotation speed determine the power output and affected by the velocity of the water flow (V), the turbine rotation speed measured in rotation per minutes (rpm) and can be calculated with Equation (5).

$$Tr = \frac{V \times \cos \times \alpha}{2} \tag{5}$$

System efficiency refers to the generator's capability to transform the kinetic energy of flowing water into electrical energy. The efficiency value is determined using Equation 6, which mathematically calculates the efficiency of the electric power generator.

$$\eta = \left(\frac{\bar{x}Pg}{Ph} \right) \times 100\% \tag{5}$$

The system are designed that the pico-hydro power plant can be carried around similar to backpack, and can be placed on motorcycle. The turbine and frame are made of Galvanised plates and hollow, whereas the electrical control panel is made of plastic. The frame have two doors that can be used to acts as a small reservoir that can increases the water velocity. The turbine specification are shown in **Table 1**. Turbine Spesificationand the frame and turbine 3D design can be seen in **Figure .**

Table 1. Turbine Spesification

Parameter	Value	Unit
Diameter	30 cm	cm
Number of Blades	16	Piece(s)
Blade Design	70°	Degree
Turbine Weight	2 kg	kg
Turbine Width	15 cm	cm
Material	Galvanism	

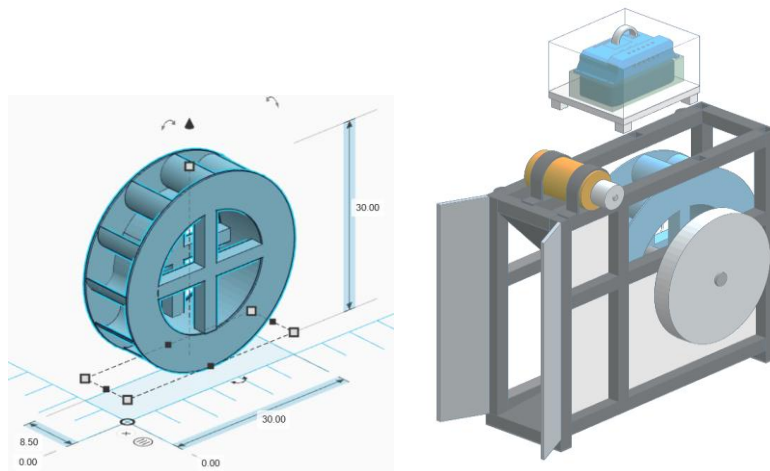


Figure 2. Turbine and System 3D Design

Table 2. Generation System Specification

Parameter	Value	Unit
Length	50	cm
Width	14	cm
Height	38	cm
Weight	15	kg
Generator Pulley	2	Inch
Turbine Pulley	6	Inch
Generator	200	Watt
SCC	10	A
Battery 3S, 4P	12	Ah
DC Lamp	12	Watt

Portable pico-hydro can generate direct current (DC) power through a 200 watts DC generator that driven by a water wheel turbine. With the pulley gear ratio 1:3 used to transfer kinetic energy from the turbine to generator. The generator generates electrical energy and then regulated by the solar charge controller, the solar charge controller can prevent backflow energy from the battery. After going through a solar charge controller, the current charge a 12V battery. With a DC power output, the system can power a DC lamp and other DC devices. The generation system specification can be shown in **Table 2**Table 2. Generation System Specification and it can be seen in **Figure .**

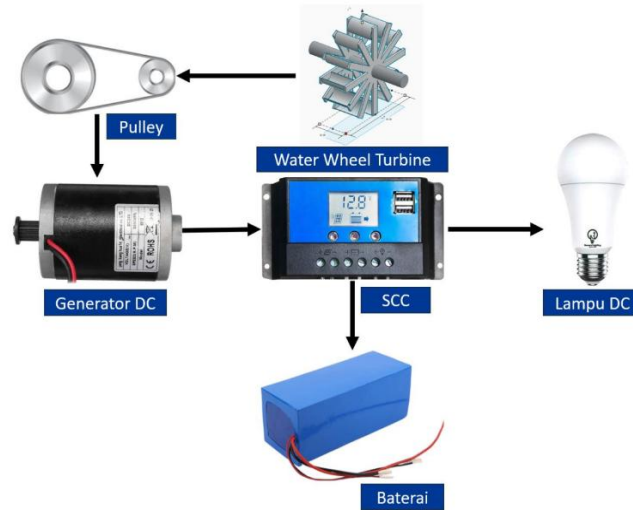


Figure 3. Power Generation System

The system is suitable to be applied in irrigation and river flow. The system are placed inclined as shown in **Figure** . The system was tested in the irrigation in Pakembinangun village and Hargobinangun village, Special Region of Yogyakarta. The portable pico hydro system's performance and efficiency will be evaluated using various methods. In the field tests, the system will be assessed under three conditions: No Load, With a 12W DC Lamp Load, and Full System (including SCC, battery, and lamp). These tests aim to observe how the generator performs both without any load and when connected to a load. Key parameters measured will include water flow rate, turbine speed (rpm), generator speed (rpm), generator voltage (volts), generator current (amperes), and power output (watts). Performance assessments will be carried out at different locations with varying water flow rates to evaluate the device's portability. Additionally, the system's durability will be tested by allowing it to operate continuously for a specified period and then examining its condition. Several methods will measure the performance and efficiency of the portable pico-hydro system. For collecting data, place the electrical box above the water flow to keep it out of the water and the turbine beneath a 10 to 15 cm water drop. The positioning during experiments significantly affects turbine rotation. The pulley ratio between the turbine and the generator is 1:3-4, meaning one pulley rotation results in three or four rotations of the generator. Both laboratory and field experiments use a multimeter for current measurement and a tachometer for the rotational speed of the turbine and generator. Field tests are conducted in three configurations: No Load, 12W Lamp Load, and Full System (SCC, Battery, Lamp). The goal of these measurements is to understand the generator's real-world performance without load and when connected to a load. Measured parameters include water flow rate, turbine speed (rpm), generator speed (rpm), generator voltage (volts), generator current (amperes), and power (watts).



Figure 4. Inclined System that Operated in Village Irrigation

3. IoT Monitoring System

The IoT monitoring system have two major components consists of hardware electronics and software with user interface. Hardware component consist of Arduino Uno R3 ATmega328P, ESP-01 module, ACS712 current sensor, DC 25V voltage sensor, 1-channel relay module, Blynk platform, push button, double-layer PCB. The Arduino Uno R3 ATmega328P was chosen for its advanced communication capabilities, making it ideal for developing reliable, responsive, and compact electronic systems. The ESP-01 module, based on the ESP8266 chip, provides wireless connectivity for devices like the Arduino Uno, enabling communication via the TX/RX serial port and allowing the creation of IoT applications dependent on Wi-Fi. The ACS712 current sensor, capable of measuring both AC and DC currents, is used for monitoring energy consumption, with enhanced sensitivity for detecting small changes. The DC 25V voltage sensor, utilizing a voltage divider principle, outputs an analog signal corresponding to the measured voltage, with adjustable accuracy. The 1-channel relay

module, operating on an electromagnetic principle, controls electrical devices such as DC lights, while the Blynk platform facilitates IoT application development, displaying monitoring data and enabling remote control via smartphones. A push button replaces traditional light switches by utilizing the bounce effect to create an electrical signal, and a double-layer PCB organizes circuit paths, minimizing the need for extensive wiring. The components will be assembled into a unified electronic design as shown in the **Figure**

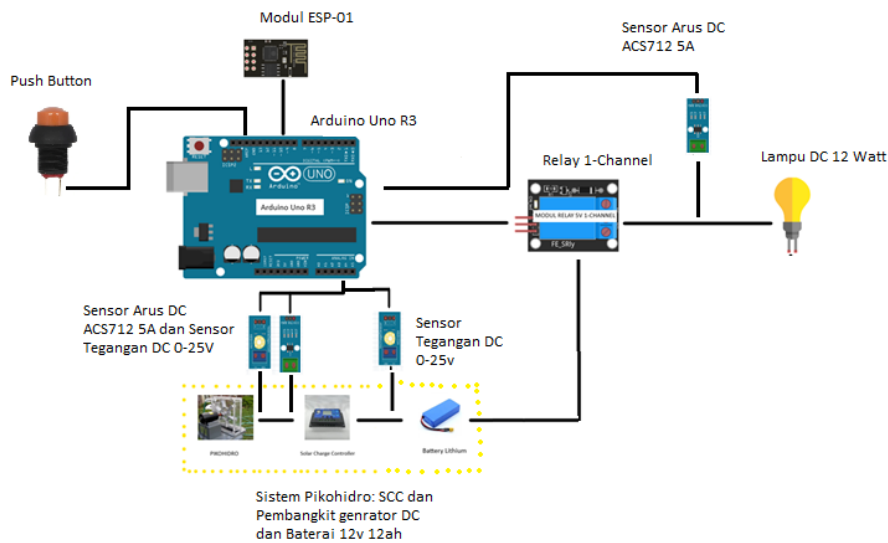


Figure 5. Electronic Design for IoT Monitoring System

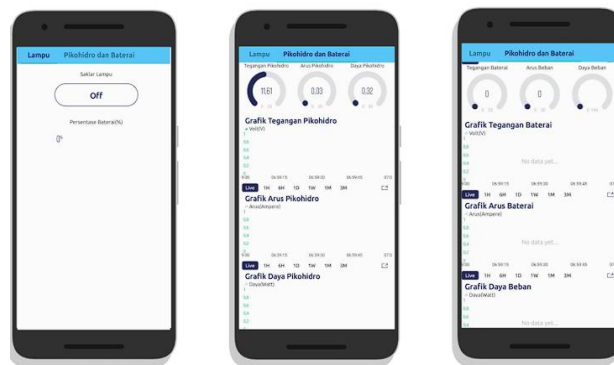


Figure 6. User Interface of Application

The PLTPH monitoring application has been designed to be accessible via a smartphone using a web-based IoT platform. The application consists of two main menus: the first menu displays a switch button and battery percentage, while the second menu shows the pico-hydro output and battery voltage, allowing users to control the lights and view a superchart graph, as illustrated in **Figure** . Application initialization is required to ensure a successful connection to the cloud server. Monitoring data is stored in Blynk's cloud, enabling access at any time. Voltage, current, and active power are displayed using gauges and superchart graphs, showing nominal values and storing them via a data logger server, while battery capacity is represented as an integer value with its corresponding nominal value. A switch button is also included for turning the DC lights on and off using a relay. The entire application can be easily designed using the Blynk IoT Platform.

In the IoT-based pico-hydro monitoring system, two measurement parameters are utilized: voltage and current. This involves connecting a DC voltage sensor and an ACS712A current sensor to the circuit between the generator and the Solar Charge Controller (SCC), connecting the DC voltage sensor between the SCC and the battery, and connecting the ACS712A current sensor in the circuit between the relay and the load. The measurements are then compared to those obtained using a multimeter to determine the percentage error for each parameter. Voltage and current readings on the generator and SCC paths are more clearly illustrated in **Figure** , where the DC voltage sensor, which has two terminals, is connected to the positive (SCC+) and negative (SCC-) cables. For the current sensor, the two terminals are connected as follows: terminal I1 to cable (G+) and terminal I2 to cable (SCC+). The wiring for the sensors is more clearly shown in **Figure** .

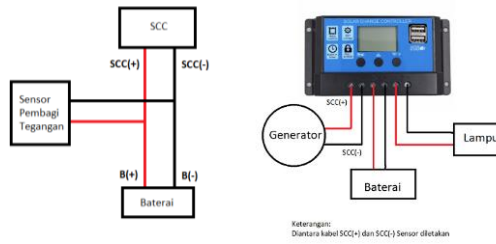


Figure 7. SCC Wiring

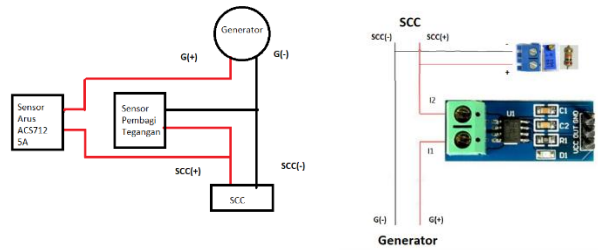


Figure 8. Wiring Measurements and Placement of Voltage and Current Sensors on the Generator

Next, the battery voltage will be measured across the SCC and the battery by connecting the DC voltage sensor to the positive (SCC+) and negative (SCC-) terminals of the generator. This setup is clearly illustrated in Figure 9. To measure the current at the load, the relay connection is established by connecting the (COM) terminal to the (SCC+). The current sensor features two terminals: terminal I1 connects to the (NO/NC) terminal, while terminal I2 connects to the (Lamp+). Additional details regarding the sensor wiring can be found in Figure 10.

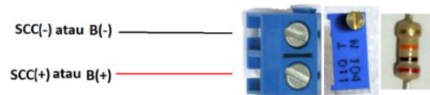


Figure 9. Wiring Voltage Sensor On Battery

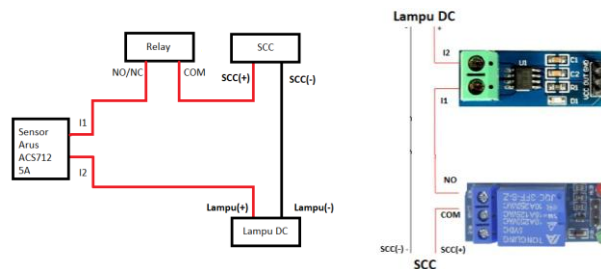


Figure 10. Wiring Current Measurement and Installation of Current Sensor, Relay on Load

The measurement process involves taking sensor readings at 5-second intervals, with three data points being collected for analysis to determine the accuracy and precision of each sensor. The sensor readings will be used to calculate the error by comparing them with the multimeter measurements taken at the same time, using Equation 3 as follows. After that, the accuracy will be calculated using Equation 4 as follows.

$$Error(\%) = \left| \frac{Nilai\ pembacaan\ sensor - Nilai\ pembacaan\ multimeter}{Nilai\ pembacaan\ multimeter} \right| * 100 \quad (Andawiyah, 2024) \quad (3)$$

$$Akurasi(\%) = 100 - Error \quad (Andawiyah, 2024) \quad (4)$$

After that, the average values of the data will be calculated using Equation 5, and the standard deviation will be determined using Equation 6. Once the average values and standard deviations are obtained, the precision can be calculated using Equation 7 as follows.

$$Mean(\bar{x}) = \left| \frac{x_1 + x_2 + \dots + x_n}{n} \right| \quad (Wildan, 2017) \quad (5)$$

Where:

Mean(x) = The average of a single data point or the midpoint

x_1, x_2, \dots, x_n = Data n

n = Number of data

$$SD = \sqrt{\frac{\sum_{i=1}^n (x_i - \bar{x})^2}{n-1}} \text{ (Wildan, 2017)} \quad (6)$$

Where:

SD = Standard Deviation

Mean(x) = Average of the data

x_i = Number of single data

n = Number of data

$$\text{Precision (\%)} = \frac{SD}{\bar{x}} * 100 \text{ (Wildan, 2017)} \quad (7)$$

The testing of battery percentage involves charging a lithium battery of 12V 12AH using a DC voltage sensor, ranging from low to high percentages, as well as discharging it using a constant current. By employing this method, the voltage will fluctuate, allowing for a comparison with voltage measurements obtained from a multimeter. To calculate the battery percentage, the following equations 8.

$$\text{Battery Percentage} = \left(\frac{V_{out} - \text{lower limit}}{\text{Upper limit} - \text{lower limit}} \right) * 100\% \quad (8)$$

Where :

V_{out} = Voltage read at the battery (sensor/multimeter) (V)

Lower limit = Lower voltage limit of the battery (V)

Upper limit = Upper voltage limit of the battery (V)

Results and Discussion

1. Performance of the Pico-Hydro System

a. No Load Test

The first field test is no load test, the purpose of this tests are in order to ensure the magnitude and stability of the voltage generated by the generator, the purpose of this test is to verify the performance under various operating conditions and confirm that the generator produces consistent and reliable output. The result is shown in Table 3 and Figure 4.

Table 3. No Load Field Test Result at Desa Pakembinangun

Rotation (rpm)		Voltage (V)
Turbine	Generator	
98	423	13.5
109	372	13.2
89	365	13
110	420	13.4
115	457	13.5
107	310	11.2
96	280	10.1
100	285	9.8
110	300	10.2
99	284	10.1

Table 4. No Load Field Test Result at Desa Hargobinangun

Rotation (rpm)		Voltage (V)
Turbine	Generator	
87	312	10.8
91	307	10.2
94	320	10.9
92	311	10.8
97	309	10.4

The testing was conducted by finding the appropriate placement position of the equipment to achieve a stable turbine rotation. The no-load experiments were carried out to ensure the voltage magnitude and stability of the generator before it enters the electrical system. Table 5 and 6 presents the no-load testing data from two locations, namely Pakembinangun Village and Hargobinangun Village. Overall, it is observed that an increase in generator rotation tends to increase the generated voltage. However, a decrease in water flow rate and changes in inclination also affect the voltage drop. The difference in locations shows voltage variations under similar conditions. This is influenced by the placement position of the equipment and the position of the water hitting the turbine.

b. 12 W DC Lamp

This experiment was conducted by directly connecting the generator to a load, which was a 12-watt lamp. The selection of the 12-watt lamp for field testing was based on the value that closely approximates the field water power, which is around 14.7 watts. The result is shown in Table 5, Table 6, and Figure 8.

Table 5. 12 Watt Lamp Test Result at Desa Pakembinangun

Rotation (rpm)		Power (W)
Turbine	Generator	
95	352	1.672
87	300	1.479
93	311	1.584
83	312	1.584
85	369	1.672
97	270	1.215
96	270	1.23
102	278	1.328
100	272	1.312
104	271	1.23

Table 6. 12Watt Lamp Test Result at Desa Hargobinangun

Rotation (rpm)		Power (W)
Turbine	Generator	
84	261	1.2
85	263	1.2
88	270	1.215
87	268	1.215
88	270	1.215

During the testing process, the lamp condition was bright and stable, with the lamp being the brightest during the experiment on July 3 in Pakembinangun. With an average flow rate of 0.015 m³/second, an average rotation of 290 rpm was achieved, and the average power output was 1.3 watts. When the experiment was conducted using an uneven belt, the lamp would dim when the uneven part of the belt was on the generator pulley. Therefore, the condition of the belt can affect the condition of the lamp/load.

c. Full System (Including SCC, Battery, and Lamp)

The overall system experiment involved the generator, solar charge controller, battery, and load. The voltage entering the solar charge controller will be limited by the solar charge controller protection system to 12.2V, and the battery will be charged by the generator. The result can is shown in Table 7, Table 8, Figure 9, and Figure 10.

Table 7. Full System Test Result at Desa Pakembinangun

Rotation (rpm)		Power (W)
Turbine	Generator	
98	356	0.732
100	358	0.732
98	350	0.488
98	353	0.488
102	354	0.61
110	315	0.11
121	340	0.46
112	317	0.111
116	322	0.224
119	325	0.23

Table 8. Full System Test Result at Desa Hargobinangun

Rotation (rpm)		Power (W)
Turbine	Generator	
88	312	1.236
82	305	1.222
86	308	1.236
91	315	1.224
83	304	1.122

From the data collected in Pakembinangun Village and Hargobinangun Village, it can be concluded that with a flow rate of 0.015 cm³/second, the generator can rotate at an average of 360 rpm and produce a voltage of 11.5V. With a flow rate of 0.015 cm³/second, the voltage and current generated are very stable because there are no changes in flow rate or other factors affecting the rotation of the turbine or generator. The field experiment results showed no impact or influence on the water flow due to the operation of the system. On closer inspection, the calculated water flow rates are quite similar, but the generator outputs differ. Several factors can influence this, including the placement position and the position of the water

hitting the turbine, the speed of the water flow, and the turbine torque. Based on the field observations with a current of 0.074 A, the battery can be charged by 0.1V over 7 minutes and 31 seconds. Therefore, it can be assumed that charging the battery from 8.25V to 12.6V would take approximately 5 hours, 8 minutes, and 11 seconds. The lamp remains bright and stable due to its power source. The efficiency of the system, based on the provided testing data and calculations, is 11.38%. This means that out of the total hydraulic power of 14.7 W generated, only 11.38% is successfully converted into electrical power by the generator, which amounts to 1.672 W.

2. Monitoring IoT Based

a. Accuracy and Precision of the System

Based on the testing conducted with the monitoring prototype for the portable pico-hydro system from the pico-hydro provider, the system utilizes several components, including a 200W-rated DC generator, a solar charge controller (SCC), a 12V 12AH battery with varying RPM, and a 12-watt light bulb. For each connection path, measurements of generator voltage and current flowing to the SCC, battery voltage, and current flowing to the load through the relay control will be taken. The results from testing with different RPMs provide various readings of voltage and current, as detailed in Tables 9 and 10.

Table 9. Voltage Reading Results from RPM Variations

RPM	Multimeter (Volt)	Sensor (Volt)	Error (%)	Accuracy(%)
100	3.14	3.08	1.91	98.09
	3.04	2.98	1.97	98.03
	3.1	3.08	0.65	99.35
150	6.23	6.23	0.00	100.00
	6.21	6.18	0.48	99.52
	6.26	6.21	0.80	99.20
200	7.64	7.65	0.13	99.87
	7.67	7.8	1.69	98.31
	7.63	7.65	0.26	99.74
250	8.54	8.63	1.05	98.95
	8.57	8.68	1.28	98.72
	8.6	8.7	1.16	98.84
300	8.71	8.72	0.11	99.89
	8.74	8.75	0.11	99.89
	8.83	8.77	0.68	99.32
350	11.9	11.9	0.00	100.00
	11.89	11.9	0.08	99.92
	11.9	11.9	0.00	100.00
400	11.9	11.97	0.59	99.41
	11.9	11.95	0.42	99.58
	11.9	11.95	0.42	99.58
450	11.96	12.02	0.50	99.50
	11.96	12	0.33	99.67
	11.96	12.05	0.75	99.25
500	11.98	12.1	1.00	99.00
	11.99	12.1	0.92	99.08
	11.98	12.07	0.75	99.25
Mean	-	-	0.67	99.33

In Table 9, 27 test data points were collected with varying RPM levels using a generator connected to the SCC and battery without a load (lamp). From these results, the accuracy and error rates of the voltage sensor readings were determined. At RPMs below 300, the error rate was 1% due to unstable RPMs, leading to inconsistent voltage readings. However, at RPMs of 300, 400, 450, and 500, the sensor readings were more consistent because the RPMs were stable, resulting in more accurate and consistent readings. The overall average error rate of 0.67% shows that the sensor performance at various RPM levels met the error tolerance specification of <10%. The results of the voltage sensor accuracy and error rates at each RPM level are detailed in Table 9.

In Table 10, 27 additional test data points were collected with varying RPM levels using the generator connected to the SCC and battery, without a load. In this case, the current measured was the current flowing into the battery. The accuracy and error rates of the current sensor readings were also analyzed. For RPMs below 300, error rates could not be calculated because the current readings were too small (<20 mA) and could not be detected by the multimeter. At 300 RPM, the error rate was relatively high, attributed to inconsistent RPMs that led to unstable current generation. At 350, 400, 450, and 500 RPM, sensor readings remained inconsistent, but the error rate was lower than at 300 RPM. With an average error rate of 10.73%, the current sensor performance across varying RPM levels did not meet the desired error tolerance of <10%. Detailed results of the current sensor accuracy and error rates at each RPM level can be found in Table 10.

Table 10. Current Reading Results from RPM Variations

RPM	Multimeter (Ampere)	Sensor (Ampere)	Error (%)	Akurasi (%)
350	0.5	0.36	28	72
	0.52	0.39	25	75
	0.5	0.36	28	72
400	0.159	0.153	3.77	96.23
	0.159	0.153	3.77	96.23
	0.159	0.152	4.4	95.6
450	0.252	0.223	11.51	88.49
	0.249	0.231	7.23	92.77
	0.254	0.243	4.33	95.67
500	0.359	0.367	2.23	97.77
	0.361	0.373	3.32	96.68
	0.362	0.388	7.18	92.82
Mean	-	-	10.73	89.27

The test results for battery voltage readings were obtained by charging a 12V 12AH battery through an SCC. The charging adapter used has a voltage of 5V and a current of 1A, with an additional charging module, as illustrated in Figure 13. The voltage readings and battery percentage can be seen in Tables 11 and 12. Table 11 presents 12 data points from the battery charging test. From these results, the accuracy and error rate of the voltage sensor readings were determined. According to the graph in Figure 11, during the charging period from 19:20 to 21:20, the error was relatively high compared to the multimeter voltage due to unstable sensor readings, which made the results inconsistent. Factors contributing to this instability include program code calibration, poor soldering of wires, and anomalies in the relay components. The average error value of 1.55% indicates that the sensor's performance during charging still meets the expected error tolerance of <10%. The error and accuracy results of the voltage sensor readings during battery charging can be seen in Table 11.

Table 11. Battery Voltage Reading Results

Time	Multimeter Voltage (Volt)	Sensor (Volt)	Error (%)	Accuracy (%)
19.00-22.40	10.69	10.73	0.37	99.6
	10.75	11.23	4.47	95.5
	11.1	11.29	1.71	98.3
	11.15	11.34	1.70	98.3
	11.18	11.39	1.88	98.1
	11.23	11.44	1.87	98.1
	11.28	11.49	1.86	98.1
	11.42	11.61	1.66	98.3
	11.88	11.98	0.84	99.2
	11.91	12.05	1.18	98.8
	11.99	12.07	0.67	99.3
	12.02	12.07	0.42	99.6
Mean	-	11.56	1.55	98.45
SD	-	0.399	-	-
Presisi (%)	-	3.45	-	-

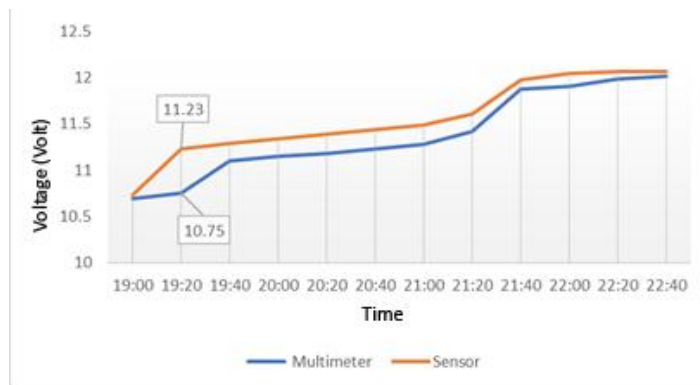


Figure 11. Battery Voltage Comparison Graph

Table 12. Battery Voltage Percentage Reading Results

Time	Multimeter Percentage Calculation (%)	Sensor Percentage Calculation (%)	Battery Percentage Difference (%)
22.00-22.00	54	55	1
	56	66	10
	63	68	5
	64	69	5
	65	70	5
	66	71	5
	67	72	5
	70	75	5
	81	83	2
	81	84	3
	83	84	1
	84	85	1
Average Battery Percentage Difference (%)			4.6

In Table 12, 12 data points were obtained regarding the battery charging percentage. The results showed the difference in the percentage of battery voltage readings, with the largest difference between the multimeter and sensor readings being 10%, which is considered significant. The average percentage difference between the two readings was 4.6%. The results also include the load current readings through the SCC while the battery was being charged. The charging adapter used provided 5V and 4A, with an additional charging module. The lamp was turned on using a relay connected to the SCC, and the current sensor measured the load current flowing through the relay. The load current readings of the 12-watt lamp are presented in Table 13. From Table 13, 21 data points were obtained for the load current. The results revealed the accuracy and error rate of the current sensor readings. According to the graph in Figure 12, the comparison between the load current measured by the multimeter and the sensor for the 12-watt lamp shows a consistent pattern. Both curves follow a similar trend, with slight differences at certain points due to sensor reading fluctuations. The sensor readings are consistent and stable, resulting in a small error, with an average error of 0.74%, indicating that the current sensor's performance meets the error tolerance specification of <10%.

Table 13. Reading Results for 12 Watt Lamp Load Current

No	Multimeter (A)	Sensor (A)	Error (%)	Accuracy (%)
1	0.371	0.373	0.54	99.46
2	0.374	0.378	1.07	98.93
3	0.381	0.383	0.52	99.48
4	0.377	0.378	0.27	99.73
5	0.372	0.373	0.27	99.73
6	0.376	0.377	0.27	99.73
7	0.369	0.368	0.27	99.73
8	0.371	0.369	0.54	99.46
9	0.376	0.374	0.53	99.47
10	0.374	0.375	0.27	99.73
11	0.372	0.375	0.81	99.19
12	0.369	0.372	0.81	99.19
13	0.368	0.370	0.54	99.46
14	0.346	0.349	0.87	99.13
15	0.342	0.338	1.17	98.83
16	0.335	0.338	0.90	99.10
17	0.359	0.355	1.11	98.89
18	0.361	0.358	0.83	99.17
19	0.355	0.351	1.13	98.87
20	0.355	0.352	0.85	99.15
21	0.359	0.352	1.95	98.05
Mean	-	0.363	0.74	99.26
SD	-	0.014	-	-
Precision (%)	-	3.78%	-	-

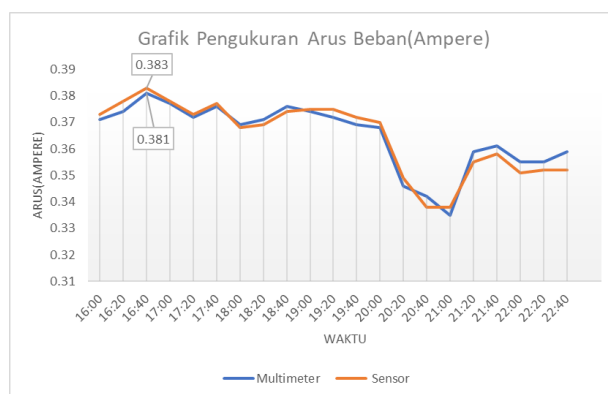


Figure 12. 12 Watt Load Current Comparison Chart

Based on the sensor readings that have been tested, the overall accuracy exceeds 95%, with precision below 4%, except for the current sensor of the generator. According to the specifications of the multimeter used, the precision for DC current readings is $\pm 2\%$, and for DC voltage readings, it is $\pm 0.5\%$. Generally, a good standard value for precision or RSD (Relative Standard Deviation) or CV (Coefficient of Variation) is $< 2\%$. This indicates that while the sensors are functioning properly and have good accuracy, their precision is suboptimal.

Conclusions

Based on the test results of the Portable Pico Hydro Power Plant (PLTPh), the designed system demonstrated that with a discharge rate of $0.015 \text{ m}^3/\text{second}$, the turbine achieved 100 rpm. Due to a pulley ratio of 1:4, the generator reached 457 rpm and produced up to 1.672 watts of power, with a no-load voltage output of 13.5V. The calculated water power was 29.4 watts, resulting in a system efficiency of 11.38%. Various specifications were adjusted to optimize the system, including modifying the dimensions, changing the generator capacity, separating the input power for measurement devices, increasing the number of turbine blades, redesigning them, and enhancing the control panel's durability. The project successfully met its goal of powering street lighting, ensuring stable and bright operation. However, the generator's battery charging performance was suboptimal, as the power output did not meet the minimum current required for fast charging, partly due to the size of the load used. The real-time data transmission time is approximately 5.64 seconds. During testing, the device achieved an IP rating of 12. Blynk is utilized for remote monitoring through its application. The designed system has an error rate exceeding 10%. It operates on a 12V DC power supply, with a total power consumption of 2.231 watts. The voltage sensor reading accuracy for the generator is 99.33% on average, with a 0.67% error rate. The current sensor reading accuracy for the generator averages 89.27%, with a 10.73% error rate. The battery voltage sensor has an average accuracy of 98.5%, with a 1.55% error rate and 3.45% precision. The load current sensor has an average accuracy of 99.26%, with a 0.74% error rate and 3.78% precision.

Acknowledgments

I would like to express my sincere gratitude to the Department of Electrical Engineering at Universitas Islam Indonesia for their unwavering support throughout this research. The resources and knowledge provided by the faculty and staff have been invaluable in facilitating my work and enhancing my understanding of electrical engineering principles. Thank you for creating an inspiring academic environment.

References

- Abdou, A. M., & Abdou, A. A. (2024). *Multi Use Water System Approach For Small Hydro Power Plants (Shpp) Alongside Irrigation And Drinking Water Supply (Dws) Networks*.
- Andawiyah, R. (2024). *[Pengukuran Analitik] Perbedaan Akurasi Dan Presisi*. Warstek.Com.
- Ashour, M. A., Abdel Nasser, M. S., & Abu-Zaid, T. S. (2023). Field Study To Evaluate Water Loss In The Irrigation Canals Of Middle Egypt: A Case Study Of The Al Maanna Canal And Its Branches, Assiut Governorate. *Limnological Review*, 23(2), 70-92.
- Balamanikandan, A., Neeraja, S. L., Kishore, T. V., Deepika, U., Prathyusha, S., & Venkatachalam, K. (2024). Iot-Enabled Advanced Health Monitoring System Using Esp32 And Ubi Dots. *2024 International Conference On Iot Based Control Networks And Intelligent Systems (Icicnis)*, 403-408.
- Calimpusan, R.-A. C. O., Arcite, L. P., & Yula, J. M. A. (2024). Design And Enhancement Of Pico Hydro And Monitoring System For Generation Of Electricity. *International Journal Of Engineering Trends And Technology*, 72(3), 49-54.
- De Zoete, N. H. (2024). *Assessing Water Allocation For Irrigation In The Brantas River Basin, Indonesia*.
- Emezirinwune, M. U., Adejumbi, I. A., Adebisi, O. I., & Akinboro, F. G. (2024). Synergizing Hybrid Renewable Energy Systems And Sustainable Agriculture For Rural Development In Nigeria. *E-Prime-Advances In Electrical Engineering, Electronics And Energy*, 7, 100492.
- Firoozi, A. A., Hejazi, F., & Firoozi, A. A. (2024). Advancing Wind Energy Efficiency: A Systematic Review Of Aerodynamic Optimization In Wind Turbine Blade Design. *Energies*, 17(12), 2919.

- Hadian, M. S. D., Suhardiman, S., Firmansyah, Y., Barkah, M. N., Sunarie, C. Y., & Ramadian, A. (2024). Water Resources Potential Assessment During Dry Season In Indonesia: A Systematic Literature Review. *Journal Of Ecohumanism*, 3(6), 1064-1092.
- Hasibuan, A., Akbar, F., Meliala, S., Putri, R., Ari Nrartha, I., & Others. (2024). Control And Monitoring Of 1 Phase Generator Automatic Voltage Regulator Internet Of Things. *International Journal Of Electrical \& Computer Engineering (2088-8708)*, 14(6).
- Hasibuan, A., Asran, A., Yanti, S., Jannah, M., Bintoro, A., & Nrartha, A. (2023). Effect Of Variation In The Number Of Blades On Turbine Rotation And Output Power At Pltph (Picohydro Power Plant) Using A Kaplan Turbine. *Bulletin Of Computer Science And Electrical Engineering*, 4(1), 49-56.
- Kandasamy, R., Ramesh, R., Natashen, R. K., Saranya, R., Suganya, T., Hiremath, K., Sb, I. A., & Bhandar, M. (2025). Investigating The Challenges Of Deploying Renewable Energy Technologies In Rural Areas. In *Addressing B5g And 6g Network Connectivity Issues In Rural Regions* (Pp. 215-238). Igi Global Scientific Publishing.
- Koondhar, M. A., Afridi, S. K., Saand, A. S., Khatri, A. R., Albasha, L., Alaas, Z. M., Graba, B. B., Touti, E., Aoudia, M., & Ahmed, M. M. R. (2024). Eco-Friendly Energy From Flowing Water: A Review Of Floating Waterwheel Power Generation. *Ieee Access*.
- Kurniawan, R., Daud, M., & Hasibuan, A. (2022). Impact Of Intermittent Renewable Energy Generations Penetration On Harmonics In Microgrid Distribution Networks. *2022 6th International Conference On Electrical, Telecommunication And Computer Engineering (Elticom)*, 30-37.
- Kurniawan, R., Nasution, A., Hasibuan, A., Isa, M., Gard, M., & Bhunte, S. V. (2021). The Effect Of Distributed Generator Injection With Different Numbers Of Units On Power Quality In The Electric Power System. *Journal Of Renewable Energy, Electrical, And Computer Engineering*, 1(2), 71-78.
- Ma, D., Belloni, C., & Hull, N. M. (2025). Innovative Microbial Water Quality Management In Water Distribution Systems Using In-Pipe Hydropowered Uv Disinfection: Envisioning Futuristic Water-Energy Systems. *Environmental Technology*, 46(7), 1045-1061.
- Quang, N. H., Viet, T. Q., Thang, H. N., & Hieu, N. T. D. (2024). Long-Term Water Level Dynamics In The Red River Basin In Response To Anthropogenic Activities And Climate Change. *Science Of The Total Environment*, 912, 168985.
- Rath, K. C., Khang, A., & Roy, D. (2024). The Role Of Internet Of Things (Iot) Technology In Industry 4.0 Economy. In *Advanced Iot Technologies And Applications In The Industry 4.0 Digital Economy* (Pp. 1-28). Crc Press.
- Siregar, W. V., Hasibuan, A., Daud, M., Puspasari, C., Hidayatullah, F., & Others. (2024). Adoption Of Renewable Energy Technology In Society For Sustainability. *2024 International Conference On Electrical Engineering And Computer Science (Icccos)*, 171-174.
- Siregar, W. V., Hasibuan, A., Hidayatullah, F., Al Farizi, R., & Others. (2024). Green Purchasing Behavior On Solar Photovoltaic Power Among Generation Z For Sustainable Energy. *Proceedings Of International Conference On Finance Economics And Business (Icofeb)*, 2, 13.
- Siregar, Y., Marbun, E. S., & Binti Mohamed, N. N. (2024). Monitoring System For Pico Hydropower Plants On Pelton Turbines Based On The Internet Of Things. *2024 8th International Conference On Electrical, Telecommunication And Computer Engineering (Elticom)*, 254-258.
- Sumarjo, J., Purnomo, S. S., Bangsa, I. A., Santoso, D. B., & Sena, B. (2024). Initial Stage Of Implementation For Hybrid Of Pico-Hydro Power And Solar Energy In Tirtasari Village, Karawang Regency. *Aip Conference Proceedings*, 3215(1).
- Teodoro, C. A. (2024). Harnessing Hydroelectric Energy From Water Irrigation Pumps: A Sustainable Lighting Solution For Agricultural Fields And Fishponds. *E3s Web Of Conferences*, 488, 2014.
- Tirtalistyani, R., Murtiningrum, M., & Kanwar, R. S. (2022). Indonesia Rice Irrigation System: Time For Innovation. *Sustainability*, 14(19), 12477.
- Usmani, S., Siddiqi, A., & Wescoat Jr, J. L. (2021). Energy Generation In The Canal Irrigation Network In India: Integrated Spatial Planning Framework On The Upper Ganga Canal Corridor. *Renewable And Sustainable Energy Reviews*, 152, 111692.
- Wildan, A. (2017). *Menghitung Standar Deviasi (Sd) Dan Standar Deviasi Relatif (Rsd)*. www.Sampling-Analysis.Com.